Aerosol direct radiative effect in cloudy scenes retrieved from space–borne spectrometers

M. de Graaf

Abstract The retrieval of the aerosol direct radiative effect of smoke aerosols in cloudy scenes using space–borne spectrometers is described. The retrieval of aerosol parameters and radiative effects from satellite is often hampered by residual clouds in a scene. However, aerosols that absorb solar radiation in the ultraviolet (UV) reduce the reflectance in the UV measured by space-borne spectrometers, and can be detected even in the presence of clouds. The absorption of radiation by small UV-absorbing aerosol disappears in the shortwave infrared (SWIR) and cloud properties can be retrieved here. This can be used to quantify the aerosol direct radiative effect (DRE) in the cloudy scene, by modelling the aerosol–unpolluted cloud reflectance spectrum and comparing it to the measured aerosol–polluted cloud reflectance spectrum. The algorithm to retrieve the aerosol DRE over clouds is applied here to SCIAMACHY shortwave reflectance measurements of marine cloud scenes. The maximum aerosol direct radiative effect found from these measurements is 124 ± 7 Wm^{-2}, which means that about 14% of the incoming solar irradiance was absorbed by the smoke aerosols.

1 Introduction

The radiative effect of aerosols is one of the least certain components in global climate models [14]. This is mainly due to the aerosol influences on clouds. Aerosols can influence e.g. cloud formation, cloud albedo and cloud life time, through their role as cloud condensation nuclei, which are called the indirect effects of aerosols [8]. But even the aerosol direct radiative effect (DRE), the component of aerosol radiative forcing that neglects all influences on clouds, is still poorly constrained, due to the heterogeneous distribution of aerosol sources and sinks and the influence

M. de Graaf
Royal Netherlands Meteorological Institute, Wilhelminalaan 10, 3732 GK, The Netherlands. e-mail: graafdem@knmi.nl

of clouds on global observations of aerosols. In particular, the characterisation of aerosol properties in cloudy scenes has proved challenging.

Modelling studies and observational evidence suggest that the DRE strongly depends on the underlying surface. Over dark surfaces like the ocean, the scattering effects of the aerosols dominate, leading to a negative DRE, while over bright surfaces and clouds aerosol absorption decreases the scene albedo, leading to a less negative or positive DRE [e.g. 6]. However, modelling studies of aerosol DRE differ in magnitude and sign, because of their strong dependence on aerosol microphysical properties used in the simulations. Aerosol microphysical properties can be found from air–borne measurements, e.g. during the SAFARI 2000 field campaign [5], or globally using satellite measurements. Aerosols significantly affect the polarised light reflected by clouds under certain scattering geometries, which can be used to derive aerosol optical properties in cloudy scenes using space–borne polarimetry measurements [13]. In the case of active remote sensing, like lidar, the atmospheric scattering properties are vertically resolved, allowing for separation of aerosol and cloud properties in a small but global track [1]. The retrieved aerosol microphysical and optical properties can be used to compute the aerosol DRE over clouds, but the accuracy of these results is strongly influenced by the accuracy of the aerosol parameters that are assumed to represent the actual aerosols.

Small aerosols, like smoke from vegetation fires, reduce the scene reflectance in the UV and visible spectral region only, which may be used to retrieve the spectral optical aerosol properties in individual cases by fitting modelled reflectance spectra to the measured spectrum [3]. However, in general a unique solution is not possible, due to the large number of aerosol properties determining the reflectance spectrum. The measured reduction of UV–reflectance can also be used directly to determine the aerosol DRE in cloudy scenes, by comparing it to a reflectance spectrum of an aerosol–unpolluted scene [10]. This avoids the need for retrieved or assumed aerosol parameters. In this chapter the aerosol DRE over clouds is derived using this method with reflectance measurements of aerosol–polluted marine cloud scenes over the South Atlantic Ocean from SCIAMACHY and modelled reflectances of aerosol–unpolluted cloud scenes. The aerosol DRE over clouds can be large over the South Atlantic Ocean in the boreal summer months (June – September), when annually recurring biomass burning events during the local dry season in southern Africa produce light–absorbing aerosols that are advected over semi–permanent marine stratiform clouds [3, 11].

2 Theory

A radiative forcing or radiative effect of an atmospheric constituent x can be defined as the difference in the net irradiance ΔE at a certain level with and without the forcing constituent [7]:

$$\Delta E_x = E^{\text{net}}_{\text{with } x} - E^{\text{net}}_{\text{without } x}, \tag{1}$$

where the net irradiance is defined as the difference between the downwelling and upwelling irradiances, $E^{\mathrm{net}} = E^{\downarrow} - E^{\uparrow}$. Therefore, at the top–of–the-atmosphere (TOA), where the downwelling irradiance is the incoming solar irradiance E_0 for all scenes, the radiative effect of aerosols overlying a cloud is given by

$$\Delta E_{\mathrm{aer}}^{\mathrm{TOA}} = E_{\mathrm{cld}}^{\uparrow\ \mathrm{TOA}} - E_{\mathrm{cld\ +\ aer}}^{\uparrow\ \mathrm{TOA}}, \tag{2}$$

where the upwelling irradiance at the TOA for an aerosol-free cloud scene is $E_{\mathrm{cld}}^{\uparrow\ \mathrm{TOA}}$ and the upwelling irradiance for an aerosol-polluted cloud scene $E_{\mathrm{cld\ +\ aer}}^{\uparrow\ \mathrm{TOA}}$. Therefore, if energy is absorbed in the atmosphere by the aerosols, the radiative forcing is positive.

The monochromatic irradiance E_λ of radiant energy is defined by the normal component of the monochromatic radiance I_λ, integrated over the entire hemisphere solid angle. In polar coordinates, this can be written as

$$E_\lambda = \frac{\mu_0 E_{0\lambda}}{\pi} \int_0^{2\pi}\int_0^{1} R_\lambda(\mu,\phi;\mu_0,\phi_0)\,\mu d\mu d\phi. \tag{3}$$

In Eq. (3), μ_0 is the cosine of the solar zenith angle θ_0, μ the cosine of the viewing zenith angle θ, and ϕ_0 and ϕ the azimuth angle of the incoming and outgoing beam relative to the scattering plane, respectively. $\mu_0 E_0$ is the TOA solar irradiance incident on a horizontal surface unit and R is the reflectance, defined as

$$R_\lambda = \frac{\pi I_\lambda}{\mu_0 E_{0\lambda}}. \tag{4}$$

The (local) plane albedo A for a scene is defined as the integral of the reflectance R over all angles

$$A_\lambda(\mu_0) = \frac{1}{\pi} \int_0^{2\pi}\int_0^{1} R_\lambda(\mu,\phi;\mu_0,\phi_0)\,\mu d\mu d\phi. \tag{5}$$

By substituting Eq. (5) in (3) and integrating over wavelength, the aerosol effect at the TOA, Eq. (2), becomes

$$\Delta E_{\mathrm{aer}} = \int_0^{\infty} \mu_0 E_0 \left(A_{\mathrm{cld}} - A_{\mathrm{cld\ +\ aer}}\right) d\lambda. \tag{6}$$

Here we have omitted the wavelength and solar zenith angle dependence of the terms on the right hand side.

The aerosol DRE over clouds can be determined using radiative transfer model (RTM) results for the first term in Eq. (6), A_{cld}, and measurements of the reflectance $R(\lambda)$ from SCIAMACHY for the second term, $A_{\mathrm{cld+aer}}$. SCIAMACHY performs contiguous measurements from 240 and 1750 nm. Therefore, the wavelength integration is also from 240 to 1750 nm.

For the simulated case the plane albedo can be obtained from the model results, by integrating the reflectances in all directions. However, for the measured case

with clouds and aerosols, only the reflectance in the measured direction is known. Therefore, the plane albedo for this scene must be estimated.

A measure for the angular distribution of the scattering energy as a function of the scattering angle for a scene is the anisotropy factor B_λ,

$$B_\lambda = R_\lambda / A_\lambda . \tag{7}$$

Assuming that the anisotropy factors are the same for the clean and polluted cloud scenes, $B_{\mathrm{cld}} = B_{\mathrm{cld\,+\,aer}}$, Eq. (6) can be written as

$$\Delta E_{\mathrm{aer}} = \int_{240\ \mathrm{nm}}^{1750\ \mathrm{nm}} \frac{\mu_0 E_0 \left(R_{\mathrm{cld}} - R_{\mathrm{cld\,+\,aer}}\right)}{B_{\mathrm{cld}}} d\lambda + \varepsilon. \tag{8}$$

The term ε contains the errors due to assumptions and measurement uncertainties. The measurement uncertainty of the aerosol DRE for SCIAMACHY was derived by applying the algorithm to aerosol–free cloud scenes. This should yield a zero aerosol DRE and differences can be attributed to systematic and random errors. Furthermore, an aerosol–polluted cloud scene was modelled using an RTM, to determine the additional errors in the algorithm from the presence of the aerosol layer. These errors were small, in the order of 1–2 Wm^{-2}. The total uncertainty of the SCIAMACHY aerosol DRE was about 7 Wm^{-2} [4].

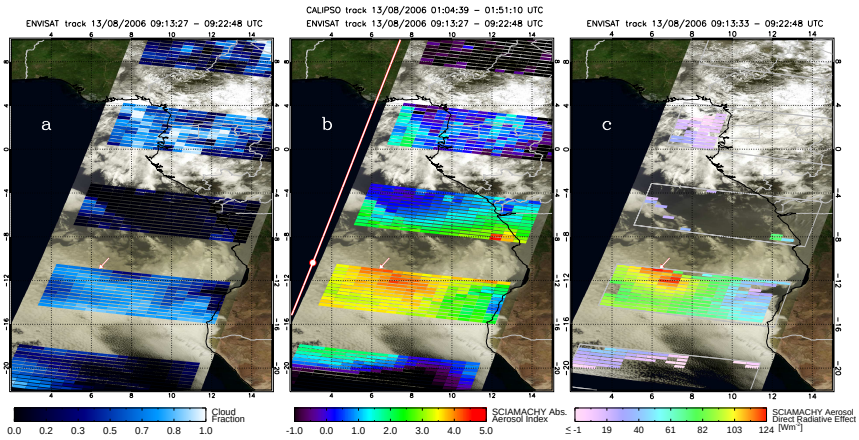

Fig. 1 MERIS RGB composite showing the horizontal cloud distribution over the west coast of Africa on 13 August 2006, from 09:13:27 – 09:22:48 UTC, overlaid with **a)** SCIAMACHY/FRESCO effective cloud fraction; **b)** SCIAMACHY Absorbing Aerosol Index; **c)** SCIAMACHY Aerosol Direct Radiative Effect [Wm^{-2}], retrieved over marine clouds only. This shows the horizontal distribution of smoke over clouds over the South Atlantic Ocean, and the subsequent positive DRE due to the absorption of radiation by the aerosols. The vertical distribution of clouds and aerosols along the white Calipso track is shown in Fig. 2. The minimum distance between the Calipso track and the selected pixel (shown by the arrow) is 300 km. The aerosol absorption in the selected pixels is shown in Fig. 3.

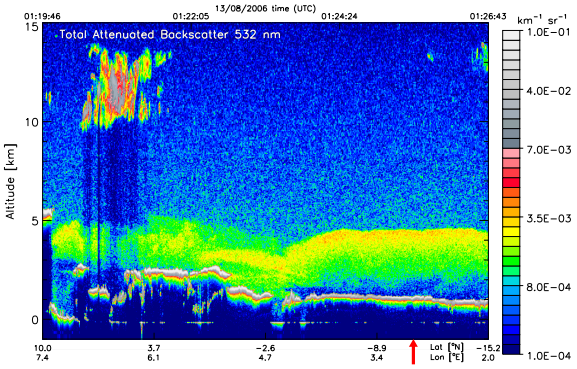

Fig. 2 CALIOP 532 nm backscatter signal on 13 August 2006, from 01:19:46 – 01:26:43 UTC, showing the vertical distribution of aerosols between 2 – 5 km (yellow/green) above clouds around 1 km (grey), along the Calipso track marked in white in Fig. 1. The red arrow corresponds to the white dot in Fig. 1.

3 Results

The aerosol DRE was derived using Eq. (8) from SCIAMACHY measurements on 13 August 2006 over the South Atlantic Ocean west of Africa. During this day smoke from biomass burning on the African mainland was drifted over the ocean in a layer between about 2–5 km altitude. Underneath this smoke layer, clouds were present over the ocean at about 1 km altitude. The horizontal distribution of the clouds and aerosols is shown by the SCIAMACHY effective Cloud Fraction in Fig. 1a and the SCIAMACHY Absorbing Aerosol Index in Fig. 1b, respectively. The vertical distribution of the clouds and aerosols along the Calipso track in Fig. 1b is shown in Fig. 2. The corresponding aerosol DRE field over marine clouds is shown in Fig. 1c, for all scenes over the ocean containing water clouds with effective cloud fractions greater than 0.3. It shows the unprecedented details of measured absorbed energy by aerosols over clouds. Clearly, the aerosol DRE is highly variable with location, dropping off to zero at the edges of the smoke field, which corresponds with the AAI gradient. The maximum aerosol DRE over clouds measured by SCIAMACHY on this day is 124 ± 7 Wm^{-2}, in the scene indicated by the arrow.

The measured reflectance spectrum for the scene indicated by the arrow in Fig. 1 is plotted in Fig. 3 in red. It shows the increase of the reflectance with wavelength for a scene with clouds and aerosols. The simulated reflectance spectrum of the aerosol–unpolluted cloud for this scene is plotted in blue. The cloud parameters were retrieved at various parts of the spectrum, as indicated. The cloud pressure and effective cloud fraction were derived using the oxygen-A band at 760 nm [12]. This cloud retrieval algorithm is not affected by aerosols overlying the clouds [13], if the aerosol optical thickness is reasonably small (smaller than about 1–2), which is the case for advected smoke layers. The cloud optical thickness and cloud droplet effective radius were retrieved at 1246 and 1640 nm, using simulated reflectances of water clouds [9]. At these SWIR wavelengths the aerosol absorption optical thickness is negligible and unbiased cloud parameters can be retrieved [4]. The total ozone column was retrieved using the ozone absorption between 325 and 335 nm [2]. The

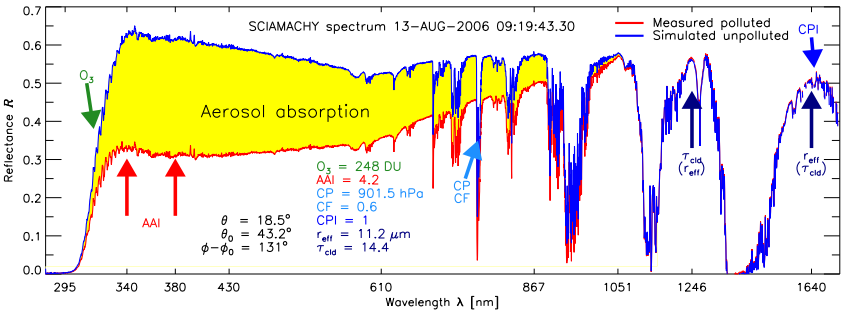

Fig. 3 SCIAMACHY measured reflectance spectrum (red) on 13 August 2006, 09:19:43 UTC of the scene indicated by the arrow in Fig. 1, and the modelled equivalent aerosol–unpolluted cloud reflectance spectrum (blue) for this scene. The difference between these two spectra (yellow, labelled 'aerosol absorption') indicates the irradiance absorbed by the aerosols (see Fig. 4). The parameters to model the cloud scene were retrieved at various parts of the spectrum (ozone (O_3 between 325–335 nm, cloud fraction (CF) and cloud pressure (CP) at 760 nm, cloud optical thickness (τ_{cld}) and cloud droplet effective radius (r_{eff}) at 1246 nm and 1640 nm). The AAI was retrieved from the reflectances at 340 nm and 380 nm.

surface albedo (not shown) was assumed to be low and constant for the ocean. Using these scene and cloud parameters, the reflectance spectrum of an aerosol–unpolluted water cloud scene can be retrieved from pre–calculated water cloud reflectance spectrum simulations [4].

The difference between the simulated aerosol–polluted cloud scene reflectance and the measured scene reflectance is large in the UV, due to the radiation absorption

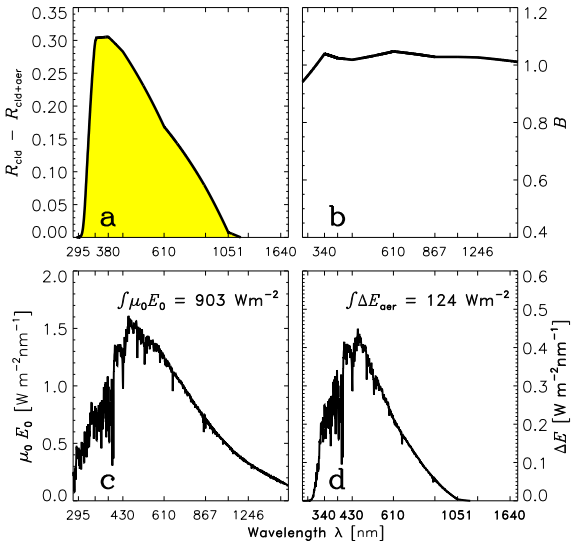

Fig. 4 The various terms of Eq. (6) to determine the aerosol DRE over clouds for the indicated scene in Fig. 1, as a function of wavelength in the SCIAMACHY spectral range. a) The reflectance difference between the modelled aerosol–unpolluted and the measured aerosol–polluted cloud scene (same as shaded area in Fig. 3); b) The anisotropy factor of the modelled aerosol–unpolluted cloud scene; c) The incoming normalised solar irradiance at TOA; d) The net irradiance change, i.e. the aerosol DRE.

by the aerosols as indicated by the yellow area. The difference disappears around 1246 nm by construction, but the measured reflectance suggests that the aerosol influence disappears already around 1100 nm.

The various terms of Eq. (8) for the aerosol DRE in the scene indicated in Fig. 3 are illustrated in Fig. 4 as a function of wavelength in SCIAMACHY's spectral range. The reflectance difference between the simulated aerosol–unpolluted cloud reflectance spectrum and the measured reflectance spectrum $(R_{\lambda,\mathrm{cld}} - R_{\lambda,\mathrm{cld+aer}})$ is given in Fig. 4a. This is the same as the yellow area in Fig. 3a. This figure clearly shows that the aerosol absorption optical thickness disappears at wavelength longer than about 1100 nm. It also disappears at wavelengths shorter than about 300 nm, because at those wavelengths all the radiation has been absorbed by ozone. This means that the SCIAMACHY spectral range suffices to capture all aerosol absorbing effects. The anisotropy factor for the modelled cloud scene $B_{\lambda,\mathrm{cld}}$ is plotted in Fig. 4b; it is typically $0.8-1.0$. The anisotropy factor for the aerosol–polluted cloud scene is not known, but a modelling study showed that the effect of an overlying aerosol layer on the anisotropy layer is small, at least for solar zenith angles smaller than 60° [4]. The normalised solar irradiance at TOA $\mu_0 E_0$ is given in Fig. 4c. The total incident solar irradiance from 240–1750 nm can be obtained by integrating the given irradiance spectrum and was 903 Wm^{-2}. The spectral irradiance change due to aerosol absorption $(E_{\lambda,\mathrm{cld}} - E_{\lambda,\mathrm{cld+aer}})$ can be obtained by combining these three terms according to Eq. (6), and is plotted in Fig. 4d. By integrating over wavelength the total aerosol DRE over clouds ΔE_{aer} was found to be 124 ± 7 Wm^{-2} for this scene.

4 Conclusions

The aerosol DRE in cloud scenes was retrieved from SCIAMACHY reflectance measurements by comparing it to modelled aerosol-unpolluted cloud reflectance spectra. The reflectance spectra of aerosol–unpolluted water clouds can be simulated using pre–computed tables of reflectances at various wavelengths. Using cloud parameters determined from the measured spectrum, at wavelengths where aerosols have no effect on the reflectance, the equivalent aerosol–unpolluted cloud reflectance spectrum for a scene can be simulated. The reflectance change in the UV due to radiation absorption by aerosols can be converted to a shortwave flux directly, which avoids the need for aerosol parameters retrievals or assumptions. This can help validate modelling results of aerosol DRE, which use the modelled radiative fluxes in an aerosol–loaded and aerosol–free scene. These results are commonly very sensitive to the assumed aerosol optical and micro-physical properties.

The SCIAMACHY measured aerosol DRE over clouds in the South Atlantic Ocean was found to be as large as 124 ± 7 Wm^{-2}, which means the aerosols absorbed about 14% of the incoming solar radiation. The measured aerosol DRE over clouds show details due to variations in the smoke and cloud fields, that can currently not be resolved by chemistry–transport models. Therefore, the measurements

from SCIAMACHY and other space–borne spectro(radio)meters may prove very valuable for understanding the radiative effects of aerosols on clouds.

The use of retrieved cloud optical thickness and cloud droplet effective radius to construct a (water cloud) reflectance spectrum implies an implicit separation of the aerosol DRE in cloudy scene from that in clear skies. This is one of the areas where observations of aerosol DRE are currently lacking [14]. Consequently, the method presented here can complement studies that retrieve aerosol parameters in clear–sky only. The latter may be used to derive the aerosol DRE in clear skies.

Acknowledgment

This work was financed by the European Space Agency (ESA) within the Support to Science Element, project number 22403.

References

[1] Chand, D., Anderson, T.L., Wood, R., Charlson, R.J., Hu, Y., Liu, Z., Vaughan, M.: Quantifying above–cloud aerosol using spaceborne lidar for improved understanding of cloud–sky direct climate forcing. J. Geophys. Res. **113**, D13206 (2008). DOI 10.1029/2007JD009433

[2] Eskes, H.J., van der A, R.J., Brinksma, E.J., Veefkind, J.P., de Haan, J.F., Valks, P.J.M.: Retrieval and validation of ozone columns derived from measurements of SCIAMACHY on Envisat. Atmos. Chem. Phys. Disc. **5**, 4429–4475 (2005). DOI 10.5194/acpd-5-4429-2005

[3] De Graaf, M., Stammes, P., Aben, E.A.A.: Analysis of reflectance spectra of UV–absorbing aerosol scenes measured by SCIAMACHY. J. Geophys. Res. **112**, D02206 (2007). DOI 10.1029/2006JD007249

[4] De Graaf, M., Tilstra, L.G., Stammes, P.: Retrieval of the aerosol direct radiative effect over clouds from space–borne spectrometry. J. Geophys. Res. *submitted* (2011)

[5] Haywood, J.M., Osborne, S.R., Francis, P.N., Neil, A., Formenti, P., Andreae, M.O., Kaye, P.H.: The mean physical and optical properties of regional haze dominated by biomass burning aerosol measured from the C–130 aircraft during SAFARI 2000. J. Geophys. Res. **108**, D13 (2003). DOI 10.1029/2002JD002226

[6] Keil, A., Haywood, J.M.: Solar radiative forcing by biomass burning aerosol particles during SAFARI 2000: A case study based on measured aerosol and cloud properties. J. Geophys. Res. **108**, D13 (2003). DOI 10.1029/2002JD002315

[7] Liou, K.N.: An Introduction to Atmospheric Radiation. Academic Press (2002)

[8] Lohmann, U., Feichter, J.: Global indirect aerosol effects: a review. Atmos. Chem. Phys. **5** (2005). DOI 1680-7324/acp/2005-5-715

[9] Nakajima, T., King, M.D.: Determination of the Optical Thickness and Effective Particle Radius of Clouds from Reflected Solar Radiation Measurements: Part I: Theory. J. Atmos. Sci. **47**(15) (1990)

[10] Stammes, P., Tilstra, L.G., Braak, R., de Graaf, M., Aben, E.A.A.: Estimate of solar radiative forcing by polluted clouds using OMI and SCIAMACHY satellite data. In: Proceedings of the International Radiation Symposium (IRS2008), pp. 577–580. Foz do Iguaçu, Brazil (2008)

[11] Swap, R.J., Garstang, M., Macko, S.A., Tyson, P.D., Maenhaut, W., Artaxo, P., Kållberg, P., Talbot, R.: The long-range transport of southern African aerosols to the tropical South Atlantic. J. Geophys. Res. **101**, D19 (1996). DOI 10.1029/95JD01049

[12] Wang, P., Stammes, P., van der A, R., Pinardi, G., van Roozendael, M.: FRESCO+: an improved O_2 A–band cloud retrieval algorithm for tropospheric trace gas retrievals. Atmos. Chem. Phys. **8**(21), 6565–6576 (2008). DOI 10.5194/acp-8-6565-2008

[13] Waquet, F., Riedi, J., Labonnote, L., Goloub, P., Cairns, B., Deuzé, J.-L., Tanré, D.: Aerosol Remote Sensing over Clouds Using A–Train Observations. J. Atmos. Sci. **66** (2009). DOI 10.1175/2009JAS3026.1

[14] Yu, H., Kaufman, Y.J., Chin, M., Feingold, G., Remer, L.A., Anderson, T.L., Balkanski, Y., Bellouin, N., Boucher, O., Christopher, S., DeCola, P., Kahn, R., Koch, D., Loeb, N., Reddy, M.S., Schulz, M., Takemura, T., Zhou, M.: A review of measurement–based assessments of the aerosol direct radiative effect and forcing. Atmos. Chem. Phys. **6**(3), 613–666 (2006). DOI 10.5194/acp-6-613-2006.